Marine and Petroleum Geology 167 (2024) 106936

Contents lists available at ScienceDirect

Marine and Petroleum Geology

journal homepage: www.elsevier.com/locate/marpetgeo

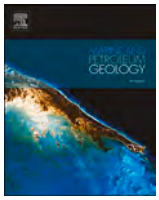

Predicting the thermal regime of the Po Plain subsurface (Italy) using geostatistical modeling constrained by legacy wells

Daniel Barrera Acosta [a], Giovanni Toscani [a,b,*], Luca Colombera [a], Chiara Amadori [a,b], Roberto Fantoni [a], Andrea Di Giulio [a]

[a] Department of Earth and Environmental Sciences, University of Pavia, Italy
[b] CRUST Centro InteRUniversitario per l'Analisi SismoTettonica Tridimensionale con Applicazioni Territoriali, Chieti, Italy

ARTICLE INFO

Keywords:
Well repurposing
District heating
Po plain
Thermal anomalies
Geothermal

ABSTRACT

Italy boasts a long history of hydrocarbon exploration. The Po Basin, in particular, has been extensively explored due to its peculiar geological setting, arising from the convergence of the Southern Alps and Northern Apennines. Because of this, substantial subsurface data have been collected and made publicly available. Today, data from past oil and gas exploration campaigns can find new life in decarbonization programs, especially for geothermal exploration. Geothermal data on the Po Basin, including bottom hole temperature (BHT) and drill stem test (DST) records, play a crucial role in understanding the thermal state of the subsurface, and can therefore be employed in the exploration of geothermal resources. This study presents a 3D model of the thermal regime in the Po Basin based on the analysis of legacy hydrocarbon wells. Geostatistical models of subsurface temperatures are produced via direct sequential simulations that consider: (i) the overall geothermal gradient across the region, (ii) anisotropy in the temperature field revealed by variogram analysis, and (iii) temperature data in the surrounding geological volumes. A base-case model of expected temperature values and associated conditional variance are thus generated from which depth-to-the-isotherm maps were extracted for temperatures in the low-enthalpy range (<100 °C). The study confirms that promising thermal anomalies are mapped in the Ferrara Arc and the buried Southern Alps. These areas offer opportunities for new developments and the repurposing of depleted oil wells for district heating. Additionally, the findings highlight other areas in the Po Plain (e.g., Emilian Arc) where there exists more subtle geothermal potential for further exploration and development.

1. Introduction

Italy has a rich history of oil and gas exploration and production, dating back to at least 1943 with the discovery of many fields in the Po Basin by AGIP, now Eni. This basin is located in northern Italy, where about one-third of the Italian population lives (ca. 20 million people), and has been one of the most prolific of continental Europe. It is a geologically very complex region because it represents the foreland basin of two opposite verging orogens: the Southern Alps and the Northern Apennines (Casero et al., 1990; Casero, 2004; Castellarin, 2001; Di Giulio et al., 2013; Toscani et al., 2014). The region experienced extension during the Mesozoic, leading to the formation of fault-bounded carbonate platforms and basins. Tectonic inversion took place since the Cenozoic in response to a compressive tectonic regime and it was followed by rapid uplift and extensive erosion of the surrounding orogenic belts during Oligo-Miocene time, and the deposition of a thick Plio-Pleistocene clastic sedimentary succession up to 7 km in thickness in the shared foreland (Livani et al., 2018; Amadori et al., 2019, and references therein). The late Cenozoic foredeep infill conceals the outermost thrusts of both the Northern Apennines and Southern Alps (Turrini et al., 2014, 2016). In this tectono-sedimentary setting, several hydrocarbon provinces were discovered associated mainly with oil and thermogenic gas in Mesozoic carbonates, and with thermogenic and biogenic gas in the Oligo-Miocene and Plio-Pleistocene successions (Casero, 2004; Cazzini et al., 2015; Fantoni, 2017; Fantoni and Franciosi, 2010). These discoveries were made mostly in the second half of the 20th century and encompassed some of the largest oil and gas fields of Northern Italy. During this time, a significant amount of subsurface data was obtained, consisting mainly of 2D seismic lines, wellbore logs, thermal data, and well cores.

However, since 2007, hydrocarbon exploration initiatives in Italy have diminished, with new discoveries encountering challenges in

* Corresponding author. Department of Earth and Environmental Sciences, University of Pavia, Italy.
E-mail address: giovanni.toscani@unipv.it (G. Toscani).

https://doi.org/10.1016/j.marpetgeo.2024.106936
Received 12 February 2024; Received in revised form 28 May 2024; Accepted 3 June 2024
Available online 6 June 2024

obtaining production approval. Consequently, the current oil and gas production in Italy predominantly relies on previously developed fields. As such, numerous wells have been abandoned, and others are approaching the end of their operational lifespan (Cazzini, 2018). Nonetheless, large amounts of subsurface data have been made publicly accessible, residing in databases such as those of the ViDEPI and Geothopica projects (Trumpy and Manzella, 2017). In this dataset, thermal data including Bottom Hole Temperature (BHT) and Drill Stem Test (DST) records, plays a pivotal role in comprehending the thermal state of the entire Po Basin. This understanding can be employed for the exploration of geothermal reservoirs and the creation of 3D geological models that integrate structural, stratigraphic, and temperature information (Sbrana et al., 2018). Therefore, it can ultimately assist both public institutions and private companies in actively seeking new sources of renewable energy.

In Europe, geothermal energy capacity doubled in the period 2010–2020 and is expected to grow even further over the next ten years according to the 2021 market report of the European Geothermal Energy Council (EGEC, 2021). The adoption of the UN Sustainable Development Goals by all United Nations member states in 2015 is driving a shift in the global energy mix towards greener, more reliable, and non-intermittent sources. The use of geothermal energy has some advantages over other renewables, like solar and wind, because of its ubiquity and capacity to provide a steady baseload. There are estimates that geothermal energy in Europe will cover 4–7% of total power generation (electricity and thermal) by 2050, with a potential increase of the European geothermal capital market of up to 210 million USD per year by the middle of the century (Dalla Longa et al., 2020). Notably, low- to medium-enthalpy geothermal energy is a readily accessible resource for heating and cooling domestic and industrial buildings. As of 2022, Italy is the fourth country in Europe by number of installed geothermal plants, in development, or planned; however, in Italy the addition in capacity over the 2010–2020 period has been modest, according to the EGEC report. For 2021, the total amount of thermal energy generated by geothermal plants was 5.885 TJ, corresponding to almost 140 ktoe (kilotonnes of oil equivalent). At present, global geothermal direct use is 58.8% for geothermal heat pumps, 18% for bathing and swimming, 16% for space heating, 3.5% for greenhouse heating, and 1.6% for industrial applications, with the rest for other applications; total energy use equals 283,580 GWh/yr (Lund and Toth, 2021). In Italy, geothermal direct use for the year 2021 reached 5.885 TJ, 41% of which was used for bathing and swimming, 21% for aquaculture, 15% for space heating (e.g., district heating), 11% for agriculture, 9% for individual heating, and 1% for industrial use (GSE, 2020). However, geothermal heat production only contributes to 2.1% of the total thermal production by renewable energy sources, and district-heating systems are the only application in Italy that is currently expanding at a sustained rate, of about 30% in terms of capacity and 8% in terms of energy used (Bargiacchi et al., 2021). Capitalizing on the substantial advantage of existing facilities, some of which are still in production, harnessing geothermal potential through the repurposing of decommissioned oil and gas wells emerges as a significant opportunity for decarbonization.

This work aims to showcase an analytical and modeling framework that provides a direct insight into potential thermal anomalies, thereby offering guidance for further exploration of geothermal resources in the Po Plain region. This is achieved by: (i) meticulously correcting all available BHT data within the Po Plain region, (ii) integrating the BHT dataset with all available DST data, and (iii) employing a geostatistical approach to build a comprehensive 3D thermal model of the entire Po Plain that accounts for the computed geothermal gradients, temperature data and anisotropy in the temperature field, and which incorporates a measure of uncertainty. From this model, we derived depth-to-the-isotherm maps, delineating the depths at which isotherms of 40 °C, 60 °C, 80 °C, and 100 °C are expected to occur.

2. Geological framework

The Po Plain is a wide alluvial valley located in Northern Italy, covering more than 40,000 km^2 and limited by the Alps to the west and the north, by the Northern Apennines to the south, and by the Adriatic Sea to the east (Fig. 1).

From a structural and geodynamic point of view, the Po Plain is located between two fold-thrust belts sharing a common foreland constituted by a portion of the Adria microplate (among others Amadori et al., 2023; Carminati and Doglioni, 2012; Dercourt et al., 1986; Toscani et al., 2014). The progressive tectonic propagation of the Southern Alps and Northern Apennines took place on a foreland affected by structures inherited from Mesozoic extensional tectonics and mainly oriented at a high angle with respect to the advancing tectonic fronts, NNW-SSE (Fantoni et al., 2004; Livani et al., 2018; Ravaglia et al., 2006; Scardia et al., 2015; Turrini et al., 2016). The two thrust-and-fold belts had different histories of tectonic activity, meaning that the Po Basin was affected by Alpine compressional tectonic events since the mid-Eocene and by Apenninic compression since the lower Miocene (Carminati and Doglioni, 2012; Maesano et al., 2015; Turrini et al., 2016; Livani et al., 2018).

In the northern and central parts of the Po Plain, the south-verging buried thrust fronts of the Southern Alps (SA), partly outcropping along the foothill zone, are present. To the south, the Pedeapenninic Thrust Front separates the outcropping Northern Apennines from the buried N-NE verging compressional structures. These buried thrusts are organized in three different structural arcs, the Ferrara Arc (FA), the Emilia Arc (EA), and the Monferrato Arc, whose geometry and rates of activity controlled the deposition and the architecture of the Plio-Pleistocene syntectonic successions of the Po Basin (onshore) and the Adriatic Sea (offshore) (Amadori et al., 2020; Ghielmi et al., 2010; Maesano et al., 2015, 2024; Panara et al., 2021 and references therein).

To date, the Plio-Pleistocene subsurface stratigraphy of the Po Basin, along with its eastward continuation in the Northern Adriatic Basin, has been characterized in some detail based on well-log correlations integrated with 2D seismic interpretation, mostly using confidential data owned by ENI. The stratigraphic framework consists of siliciclastic units bounded by regional-scale unconformities and correlative conformities of different orders. The sedimentary sequences and related unconformities bounding them are produced by the interplay of the Northern Apennines fold-thrust belt compressional tectonics, which led to the creation of new foredeep depocenters and the deformation of previous ones, with Plio-Pleistocene climate-driven sea-level changes (Ghielmi et al., 2010, 2013; Amadori et al., 2019). These boundaries can be recognized in wells and seismic reflection profiles based on abrupt facies changes, showing that the Apennine orogenesis and climate strongly influenced sedimentation rates by controlling the elevation of basin margins, erosional conditions, the extension of the drainage areas, and the shape and depth of deep-water depocenters. Since the end of the Messinian Salinity Crisis (Rossi et al., 2015; Amadori et al., 2018a, 2018b) and throughout the Pliocene, a deep narrow, and cylindric foredeep evolved parallel to the northern Apennine orogen, allowing the deposition of fine-grained turbidites. By contrast, on the northeastern side of the foreland (the Northern Adriatic-Venetian area), coarse-grained southward-prograding alluvial systems developed (Stefani, 2002; Stefani et al., 2007; Tosi et al., 2015; Toscani et al., 2016; Mancin et al., 2016; Amadori et al., 2020).

The Pleistocene was instead characterized by a stepwise evolution related to the last and intense phase of Apennine migration, which caused the separation of the cylindric Pliocene foredeep in two deep depocenters. A km-deep piggyback basin evolved behind the Ferrara arc, which was completely infilled during the middle-late Pleistocene when the paleo-Po River sediment wedge initiated eastward progradation. This period corresponds to an important change in the history of infill of the Po Basin, marked by a shift from marine to continental sedimentation, which was in part associated with the onset of the major Alpine

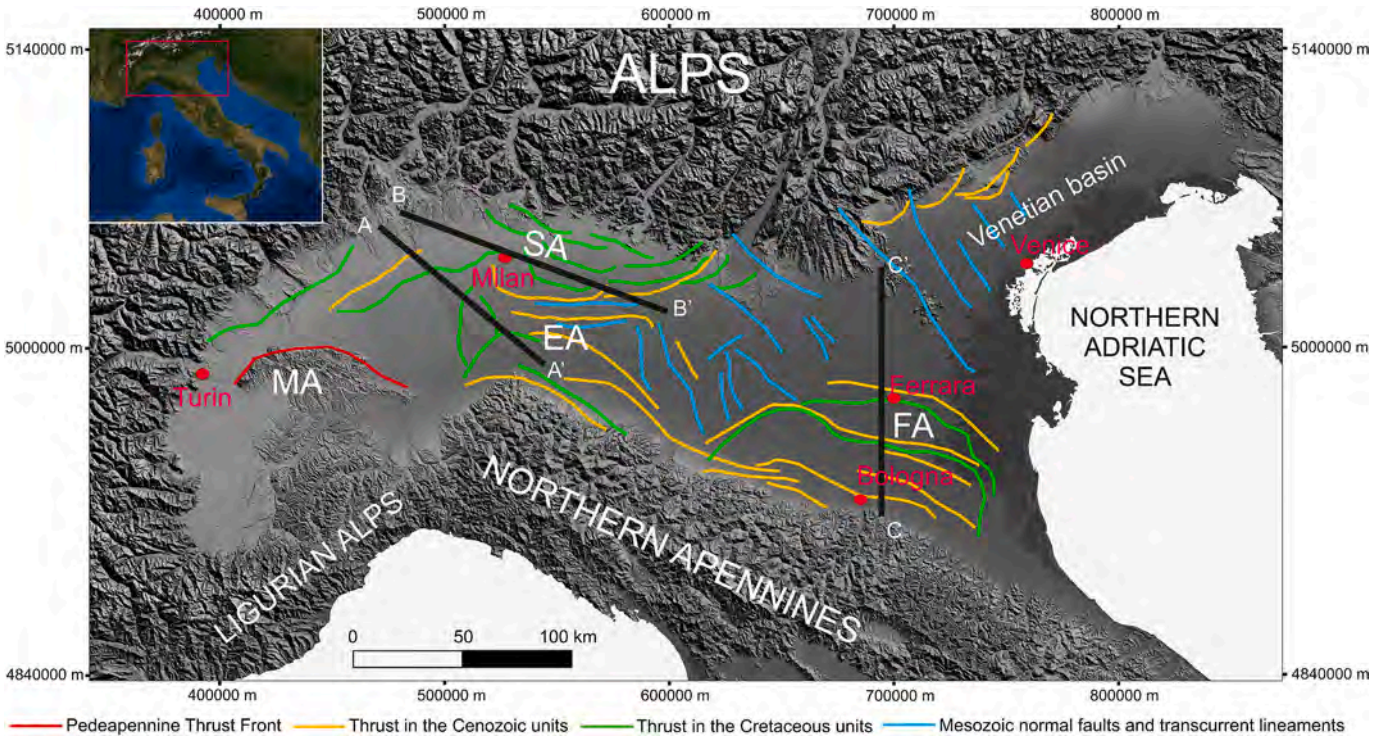

Fig. 1. Structural setting of the Po Plain subsurface in northern Italy. Faults are color-coded according to the age of the units involved in the deformation (adapted after Scardia et al., 2015; Turrini et al., 2016; Ghielmi et al., 2013). Sections A-A′ to C–C′refer to geologic sections adapted and modified from Fantoni and Franciosi (2010) and referred to later in this work. FA: Ferrara Arc, EA: Emilia Arc, SA: Southern Alps buried thrusts, MA: Monferrato Arc.

glaciation (at ca. 0.9 Ma according to Muttoni and Rogledi, 2003). Deposition of this middle-late Pleistocene continental, dominantly fluvial, succession resulted in the compensation of previously articulated morphologies, by overfilling the available accommodation space onshore and forcing the progradation of the active depositional systems towards the northern Adriatic Sea.

3. Dataset and methodology

3.1. Wells

In this work, the main data source was the Geothopica project website (Trumpy and Manzella, 2017; https://geothopica.igg.cnr.it/), a publicly available database containing thermal data that was originally part of the National Geothermal Database created in 1993 by the International Institute for Geothermal Research in Italy. The database was later revised and digitized by the CNR Institute of Geosciences and Earth Resources of Italy with the support of ENI, and eventually rendered

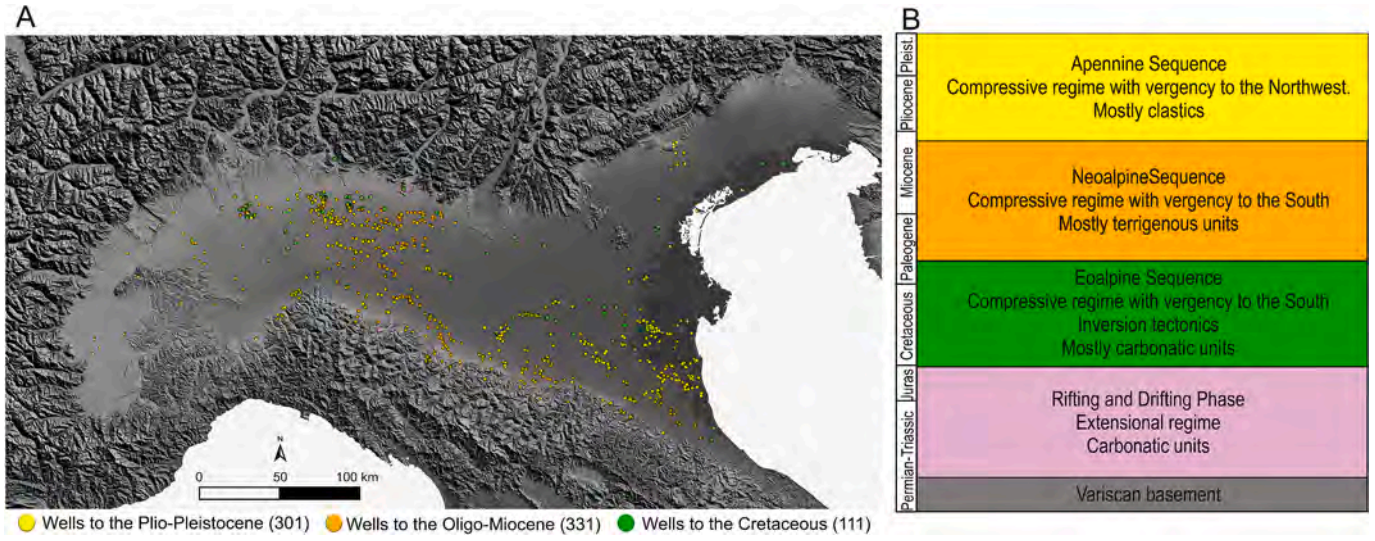

Fig. 2. (A) Location of wells with thermal data used in this research, color-coded according to the age of the deepest units drilled by the borehole. The numbers in brackets indicate the number of wells with a bottom hole reaching each unit. (B) Simplified stratigraphic scheme of the Po Plain subsurface; modified from Fantoni and Franciosi (2010).

available as an online open-access tool. The Geothopica dataset was integrated with data coming from the ViDEPI project database (https://videpi.com), created by the Italian Geological Society as a tool for making documents on Italian oil exploration publicly accessible; the data include Formation Evaluation Logs and Final Well Logs with coordinates, and the stratigraphy obtained from mudlogging.

We selected the wells with temperature data in the Italian regions of Piemonte, Lombardia, Emilia Romagna, and Veneto, accounting for a total of 743 wells. From those, a total of 1647 bottom hole temperature (BHT) and 84 drill stem test (DST) records with direct temperature measurements were obtained. The stratigraphic data were analyzed to differentiate the units reached by each well, e.g., the Plio-Pleistocene, Oligo-Miocene, and Carbonate units (Eocene-Cretaceous) (Fig. 2).

3.2. Temperature calculation

It is a standard procedure while working with thermal data from boreholes to perform corrections to the measurements taken using the Bottom-Hole Temperature (BHT) method, because of the nature of the measurement process, which involves obtaining readings at the bottom of the drill hole after the perforation. This procedure induces a modification to the formation temperature due to the cooling effect caused by the perforation mud. Several methods have been proposed to correct BHT data, but the most used is the one proposed by Horner (1951), which considers the dimensions of the borehole, parameters from the perforation, and the physical properties of the drilling mud. A general equation for temperature correction in the Po Plain as a function of depth, using the Hornet method, was proposed by Pasquale et al. (2008). To perform this correction, it is necessary to know: (i) the shut-in time, that is, the time elapsed between the end of mud circulation and the temperature measurement, and (ii) the time the mud has been circulating inside the well. The equation used to correct the BHT data is as follows:

$$T = BHT + (az - bz^2)\, ln\left(1 + \frac{T_c}{T_e}\right) \quad (1)$$

where T is the corrected temperature formation, BHT is the temperature measured at the bottom of the hole, z is the depth of the measurement, T_c is the mud circulating time and T_e is the shut-in time. Different values are recommended for coefficients a and b for the Pedealpine area and the Apennine area overlying buried thrusts, with values of a = 18.9, b = 2.7 and a = 16.0, b = 2.1, respectively (Pasquale et al., 2008). Pasquale et al. (2008) also stated that improved accuracy can be achieved by increasing the equation results by 2 °C when $T_e < 10$ h. The analyzed database provided an extensive amount of data on circulation times, but values were missing for some of the wells. In these cases, the T_c was calculated using equation (2), proposed by Pasquale et al. (2008).

$$T_c = 1.7 + 0.05z + 0.10z^2 \quad (2)$$

These corrections were applied to each well in the database, selecting the longest shut-in time where two different measurements were taken at the same depth. The DST data were obtained from several oil fields, where hydrocarbons were in production, and the reservoir fluid temperature is assumed to be in equilibrium with the temperature of the surrounding formations.

Although there is uncertainty in the calculated temperatures, the extensive horizontal and vertical coverage of the database helps mitigate the bias in estimations of average thermal gradients (Deming, 1994).

3.3. 3D geocellular model of the subsurface temperature field

A three-dimensional model of the subsurface temperature field in the Po Basin has been constructed based on the integration of: (i) the overall geothermal gradient across the region, (ii) anisotropy in the temperature field revealed by variogram analysis of the corrected borehole temperature data, and (iii) temperature data in the surrounding geological volumes treated as hard data for model conditioning. The model has been built via geostatistical simulations of the temperature values, which produced fifty equiprobable realizations of the subsurface temperature field, thereby enabling extraction of a base-case 3D model as well as a measure of variability-related uncertainty.

The average geothermal gradient across the region can be described by a linear relationship relating corrected temperature values to depth (Fig. 3) This trend has been employed as a soft constraint in the geostatistical model to force the expected non-stationarity in the temperature field. Anisotropy in subsurface temperatures has been characterized by the computation of an experimental variogram, which exhibits a larger range for the foreland-parallel direction (i.e., approximately E-W) as opposed to the cross-foreland direction; as expected given the scale of investigation and geothermal gradient, a variogram sill cannot be identified for the vertical direction. An anisotropic variogram model has therefore been employed for geostatistical modeling (range values of 18 km and 14 km, for E-W and N–S directions, respectively). Fifty equiprobable realizations of the temperature field have been generated via 3D geostatistical simulations performed over a Cartesian geocellular grid with a horizontal resolution of 1 km and vertical resolution of 10 m. The direct sequential simulation method has been applied, which allows the specification of a uniform (i.e., box-shaped) temperature distribution (Caers, 2000): the DSSIM algorithm in the SGeMS software platform

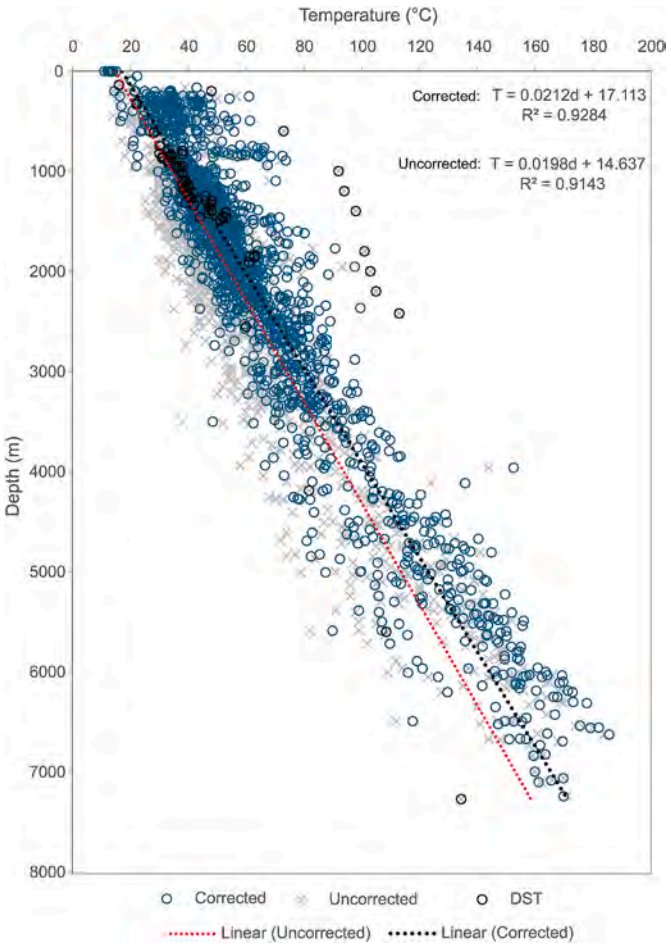

Fig. 3. Scatterplot of temperature versus depth including original BHT data, corrected BHT data, and DST data. The dotted red line shows the least-square regression curve for the uncorrected data while the gray line shows the regression based on the corrected values. Note that most of the DST values occur along the regression curve for the corrected BHT data. In the regression equations, T stands for Temperature (°C) and d stands for Depth (m).

has been used (Remy et al., 2009). Through direct sequential simulations, temperature values are assigned to each cell stochastically by considering (i) conditioning data consisting of all corrected temperature readings contained in an ellipsoidal search neighborhood of 20 km × 20 km (horizontally) x 5 km (vertically); (ii) the linear trend describing the regional average geothermal gradient, integrated into the simulation via kriging with a locally varying mean; (iii) the aforementioned variogram model.

The resulting fifty realizations have been synthesized by computing a conditional expectation estimate of the temperature field by averaging all simulation outputs; the associated conditional variance is also obtained as a measure of uncertainty in the simulated outputs. This was done using the simulation postprocessing utility in SGeMS (Remy et al., 2009). In a model of this type, areas of the model that are located further away from conditioning data (boreholes) tend to be characterized by geothermal gradients that are more likely to approximate a simple linear

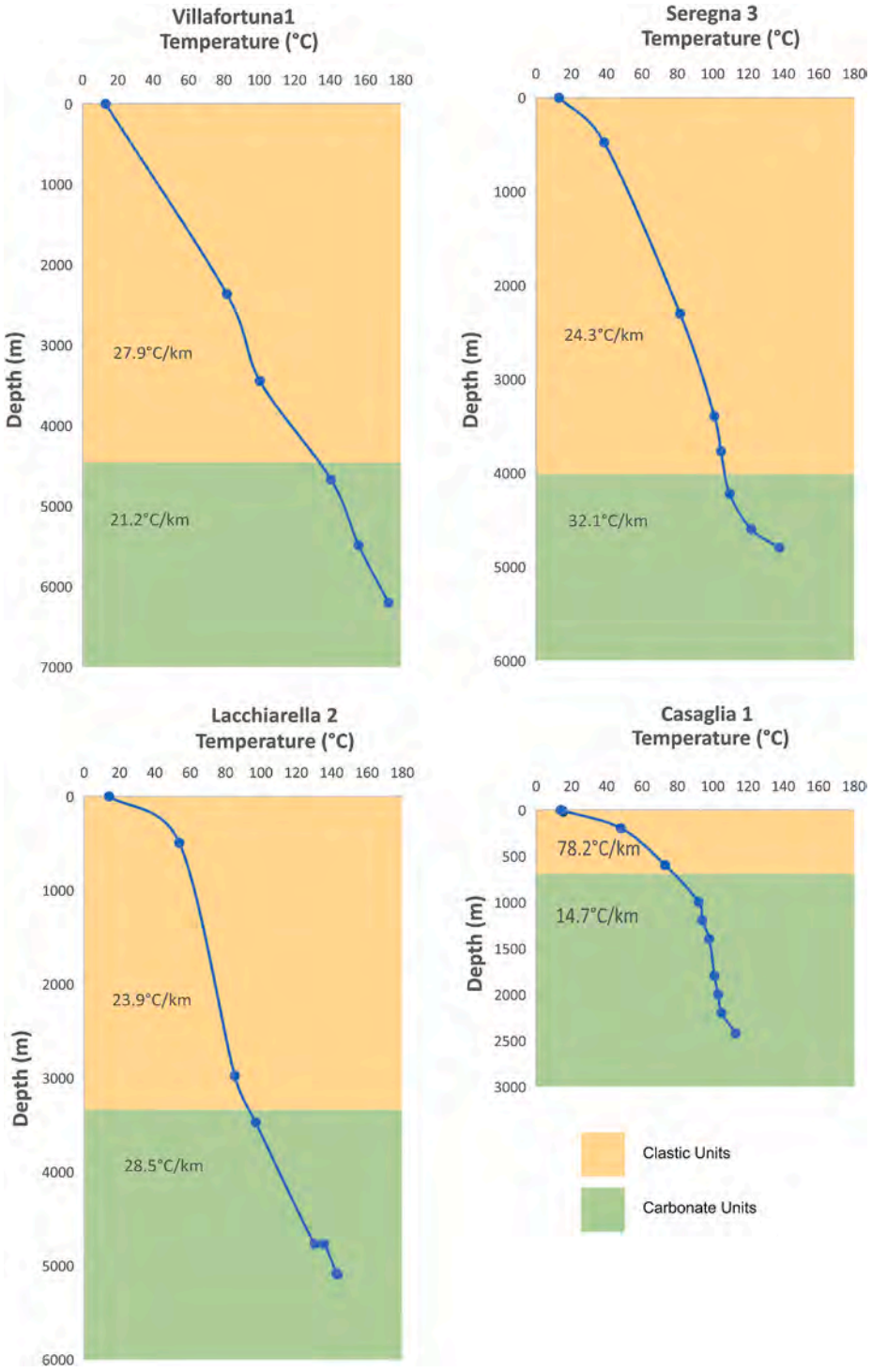

Fig. 4. Borehole temperature data showing relationships between geothermal gradient and broadly defined lithological units. Black horizontal line indicates the top of the carbonates, indicating the boundary between the clastic units (Oligocene to Pleistocene) and the carbonate units (Eocene-Cretaceous). Note the variation of gradient between units. Villafortuna 1 and Seregna 3 belong to the Southern Alps zone, Lacchiarella 2 to the Emilian Arc (Northern Apennines) and Casaglia 1 to Ferrara Arc (Northern Apennines).

trend; however, these same areas are also characterized by higher uncertainty (conditional variance).

4. Results

The geothermal gradient calculations performed using all the thermal data compiled and corrected for the Po Basin yield an average regional value of 21.2 °C/km; a gradient of 19.8 °C/km can instead be derived from the uncorrected data. The majority of the DST data falls along the regression line of the corrected thermal data, highlighting the accuracy of the method used for correction (Fig. 3). It should be noted however that the gradient shows a non-linear pattern in some of the deeper boreholes. To better understand this gradient variation with depth, a more detailed analysis was carried out in wells with a larger record of thermal data along their profile, distributed along the three different arcs, such as wells Casaglia 1 (FA), Villafortuna 1 (SA), Seregna 1 (SA) and Lacchiarella 2 (EA). The Casaglia 1 well displays a regression in the geothermal gradient, with a gradient of 78.2 °C/km in the Oligo-Miocene units and a gradient of 14.5 °C/km in the Carbonate units. The same regression of the gradient occurs in the Villafortuna 1 well, although with a smaller difference between the clastic and carbonate units (Fig. 4) The Lacchiarella 2 and Seregna 3 wells display an increase in the geothermal gradient where they penetrate the carbonates, with a gradient of 23.9 °C/km and 24.3 °C/km respectively in the clastic units, and an increased gradient of 28.5 °C/km and 32.1 °C/km, respectively, in the carbonate units. These variations in geothermal gradient are associated with the occurrence of positive anomalies, which appear to be related to carbonate tops located at shallower depths. The regional average geothermal gradient based on corrected temperature readings was used to impose a general trend in the geostatistical model; notwithstanding, the conditioning temperature data give rise to local variations in the geothermal gradient, enabling the prediction of temperature inversions and anomalies.

Maps of the depth to specified isotherms (Fig. 5) can be extracted from the geocellular grid of the expected values of temperature obtained by averaging the geostatistical simulations. The depths reported in these maps are based on a 3D temperature model (Fig. 6), and therefore consider temperature data in 3D, including data that may be associated

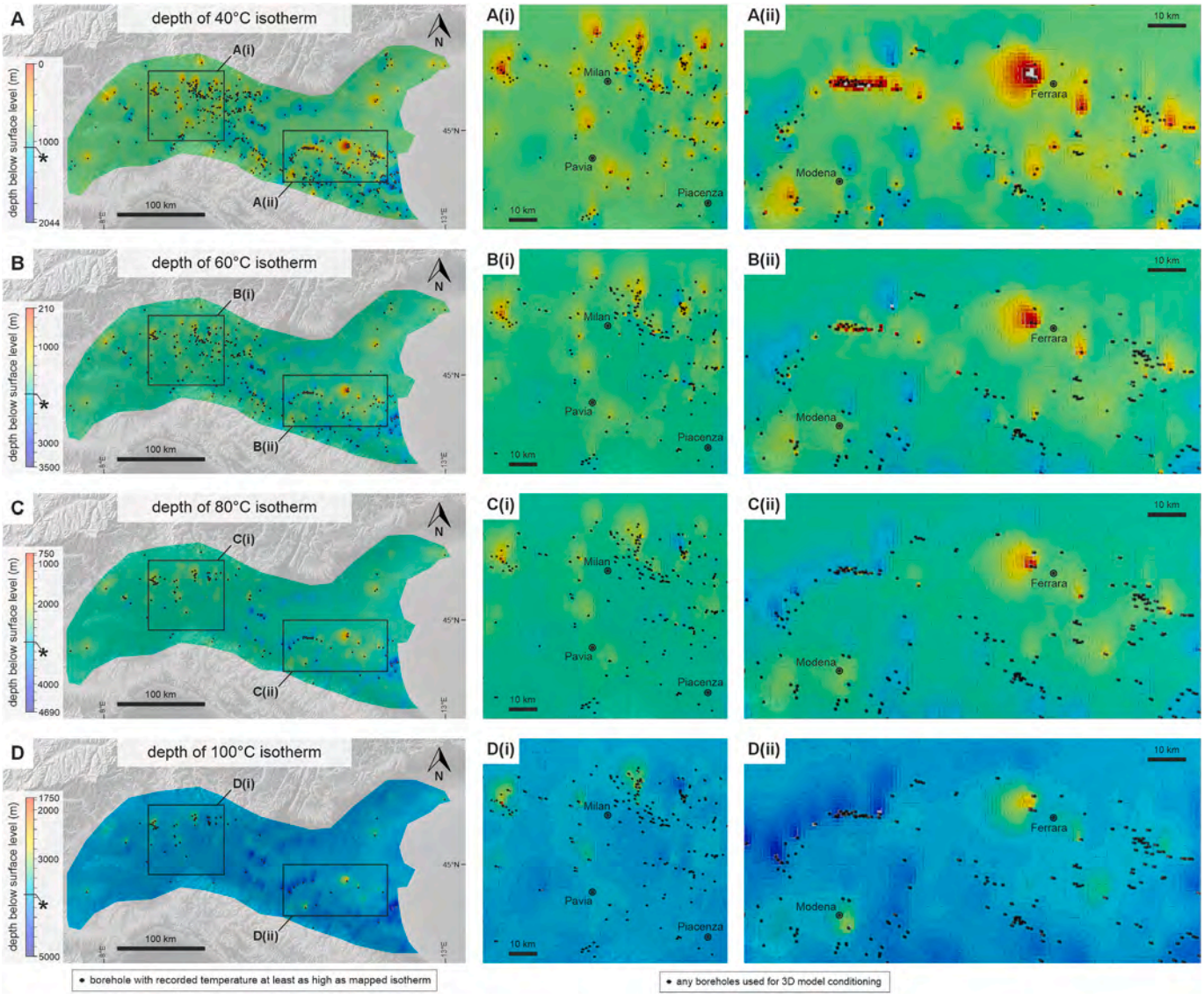

Fig. 5. Depth-to-the-isotherm maps for 40 °C (A), 60 °C (B), 80 °C (D), and 100 °C (D). For A, B, C, D, the asterisk denotes the depth at which the temperature is expected based on the regional geothermal gradient alone. A(i), B(i), C(i), D(i), display a close-up in the major anomalies found in Southern Alps. A (ii), B(ii), C(ii), D (ii), display a close-up in the anomalies found in the Ferrara Arc (Northern Apennines). These surfaces are not merely obtained through interpolation of observations: they are extracted from a 3D grid of the conditional expectation estimates of the temperature field simulated geostatistically.

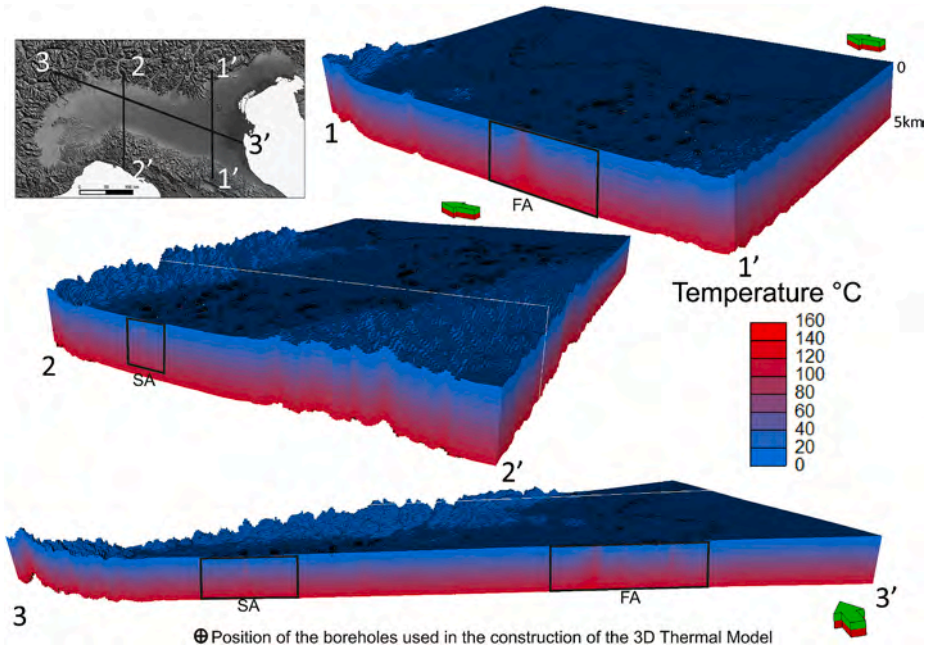

Fig. 6. Tridimensional geocellular thermal model showing the conditional expectation estimates of the temperature field in the basin, conditioned on BHT and DST data obtained from the oil and gas wells. Black frames indicate principal anomalies and their regional extension, as well as other minor anomalies. Positive anomalies in 1-1′ through the Ferrara Arc and in 2-2′ associated with the Southern Alps buried thrusts. Both anomalies are also seen in section 3-3'. Note the ×5 vertical exaggeration on the sections, which renders thermal anomalies with a peak-like geometry when in reality, these anomalies could be wider than 10 km with a more elongated geometry.

with wells that do not penetrate to depths at which the particular temperature of interest is observed. The 3D model integrates (i) the regional geothermal gradient, employed as a base trend, (ii) variogram analysis of the well data, which captures anisotropy in the temperature field arising from geological controls (primarily, trend of thrust faults and orientation of related anticlines), and (iii) the corrected temperature data, which reflect local hydrogeological control on geothermal plumbing systems (e.g., presence of faults acting as flow conduits). In this regard, these maps differ fundamentally from analogous maps that are merely obtained via 2D interpolation across wells. These maps can be employed to predict the likely depths at which it is possible to find certain temperatures at any given point in the Po Plain. In these maps, for instance, it is possible to identify the positive thermal anomaly associated with the Ferrara Arc, in correspondence of which a 100 °C isotherm can be found at depths as shallow as 1.7 km (Figs. 5 and 6). Other positive thermal anomalies can be found in association with the Southern Alps thrusts, with the shallowest depth for the 100 °C at about 3 km. Other local, deeper anomalies can be identified to the west of the Emilia Arc and to the north-east in the Venetian Plain.

To demonstrate how the produced geothermal model can assist characterization of geothermal resources in the shallower sedimentary units, where low-enthalpy geothermal solutions are more suitable, we have evaluated the temperature distribution along the base of the Pliocene. The expected temperature distribution at each point on the base of the Pliocene was obtained by intersecting the 3D temperature model with the surface (Fig. 7). These outputs enable analysis of temperature values predicted on horizons of interest, as well as their deviations relative to values expected based on the regional geothermal gradient, both in vertical profiles and in planform (Figs. 7 and 8).

The geocellular model of subsurface temperature also allows improved investigation of potential relationships between geological structures and thermal anomalies. To show this, regional geological cross sections (adapted from Fantoni and Franciosi, 2010) were projected on sections of the thermal model (Fig. 9). Such a model also permits 3D mapping of the temperature field in geological volumes surrounding wells that show a local inversion in the geothermal gradient, which, especially within the shallow subsurface (hundreds m depth), may be associated with hydrogeological controls.

Section A-A' (Fig. 9) shows a NW-SE transect between the SA (Villafortuna 1 well) and the EA (S. Cristina Bissone 1 and Turro 3 wells) crossing an inversion structure (Lacchiarella 2 well) below the depocenter of the EA, to the west. In this transect, a local thermal anomaly is shown that is associated with the structural high from the VillaFortuna-Trecate oil field to the NW. A lower-grade thermal anomaly can be found associated with the inversion structure of the Lacchiarella field. In general, limited temperature variability is observed along the EA, even though the section crosses the structural highs of the San Colombano and Stradella anticlines, drilled by the S. Cristina Bissone well and Turro well, respectively.

Section B–B' (Fig. 9) intersects the main structures of the SA, such as the Seregna, Malossa and Cigole structures. Here, the main detachment is located in the Oligo-Miocene units, but some thrusts are connected with deeper thrusts cutting upwards through carbonate units. Thermal anomalies are located above the main structures and associated with the tip of the main thrusts. No significant deviation is observed for the isotherms around the well Soncino 1, where the top of carbonate units reaches depths of more than 7 km. The well Varedo 1 shows an inversion in the thermal regime at very shallow depths, possibly associated with local hydrogeological controls.

Section C–C' (Fig. 9), located in the proximity of the Ferrara Arc, shows the largest thrust displacement, which has brought the carbonates to maximum depths of less than 1 km in the outer arcs. In this context, more widespread thermal anomalies can be found located right above the structural highs presenting carbonates at their cores, as shown in the well Casaglia 1. The well Baricella 1 displays a subordinate anomaly associated with Oligo-Miocene thrusts with detachments located in carbonate units at higher depths; hydrothermal fluids might have migrated via those faults into the anticlines.

5. Discussion

Previous approaches to the characterization of temperature

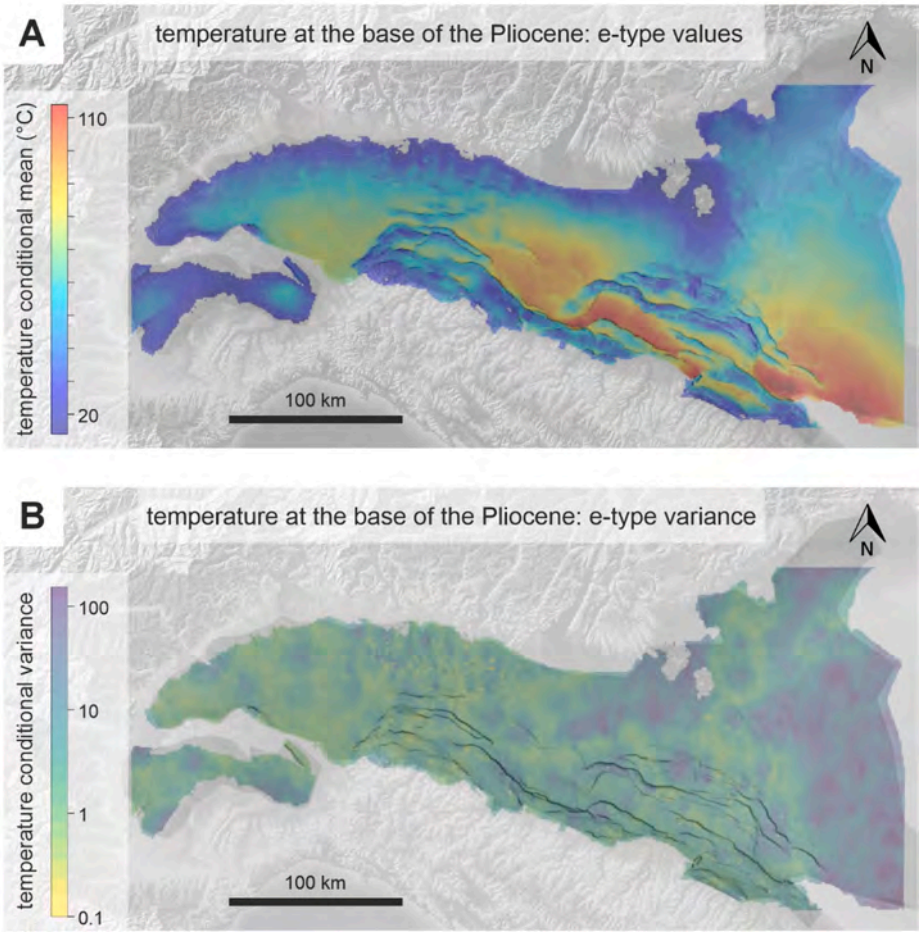

Fig. 7. (A) Expected temperature values at the base of the Pliocene, constructed by intersecting the stratigraphic surface with the 3D geocellular model of the temperature field. (B) Conditional variance in simulated temperature values on the base of the Pliocene.

variations in the Po Basin were focused on establishing the temperatures reached over 0.5 km–3 km depths (Cataldi et al., 1995; Bertani and Magrini, 2000; Trumpy and Manzella, 2017). Other approaches to creating depth to the isotherm maps have been carried out for local studies in the Ferrara Arc, around the cities of Ferrara and Mantova (ISPRA, 2015; Torri et al., 2015). For the first time, a comprehensive correction of all available borehole thermal data has been undertaken. Corrected temperature data and results of their analysis (variography, regional geothermal gradient) have been employed in a geostatistical framework to produce a tridimensional geocellular model of the temperature field in the basin. From this model, the depth of specified isotherms can be extracted at any point, to aid geothermal exploration by better delineating basin-wide variations in prospectivity. By compounding results from multiple possible realizations of the temperature field, the expected temperature distribution along specified geological features (e.g., along the base of the Pliocene; Figs. 7–8) can be coupled with a measure of the uncertainty in the predicted temperature. The predicted temperatures (cf. Fig. 8) exhibit significant local deviations from the average geothermal gradient, highlighting anomalies that must be explained by geological controls. This model portrays the well-known thermal anomaly of Ferrara (Pasquale et al., 2013; Rapti and Caputo, 2021), providing a full 3D characterization of the magnitude of the anomaly (ca. 10 km wide); yet, the model also demonstrates the existence of other positive anomalies in the area, close to the city of Modena and east of Ferrara, with temperature values above the FA that are considerably higher at shallower depths compared to any other locations. The model also predicts lower-grade positive anomalies in the SA domain, north and west of Milan. Conversely, the main thrust system of the EA is characterized by a geothermal gradient that is comparable with the regional average and by a lack of notable anomalies associated with geological structures, except for a minor anomaly north of Pavia (Fig. 5). To better understand the mechanisms controlling these anomalies and their magnitudes, it is necessary to compare the characteristics of the temperature field with geological features and the geological evolution of each sector of the basin (Figs. 7 and 9). From this comparison, it is possible to note that the SA buried thrusts exhibit a detachment mainly in the Oligo-Miocene units; however, some thrusts are connected with deeper faults cutting upwards from the basement and involving the carbonate units. In the FA area, the detachments involve the basement and extend structurally into the Pleistocene; yet, they also involve carbonate units at the core of the anticlines, displacing them at depths as shallow as 0.5 km in the frontal thrusts. The EA, on the other hand, is characterized by a thick succession of Plio-Pleistocene units above an even thicker Oligo-Miocene stratigraphy overlying deeply seated carbonate units, located at depths of about 6–7 km; however, in its associated western depocenter, a thinner sequence of Oligo-Miocene units can be found due to a structural high with raised carbonate units displaced by inversion of previously normal faults, which controlled the evolution and geometry of the arc (Livani et al., 2018). Outside of the arcs, the main depocenters tend to have a geothermal gradient lower than the average, yielding temperatures of around 50–60 °C at 3 km depth. These values, below the temperatures expected on the basis of the average geothermal gradient, are probably due to the thermal properties of the thick sedimentary succession and the absence of tectonic structures.

Previous studies (Cataldi et al., 1995; Pasquale et al., 2013; Rapti and

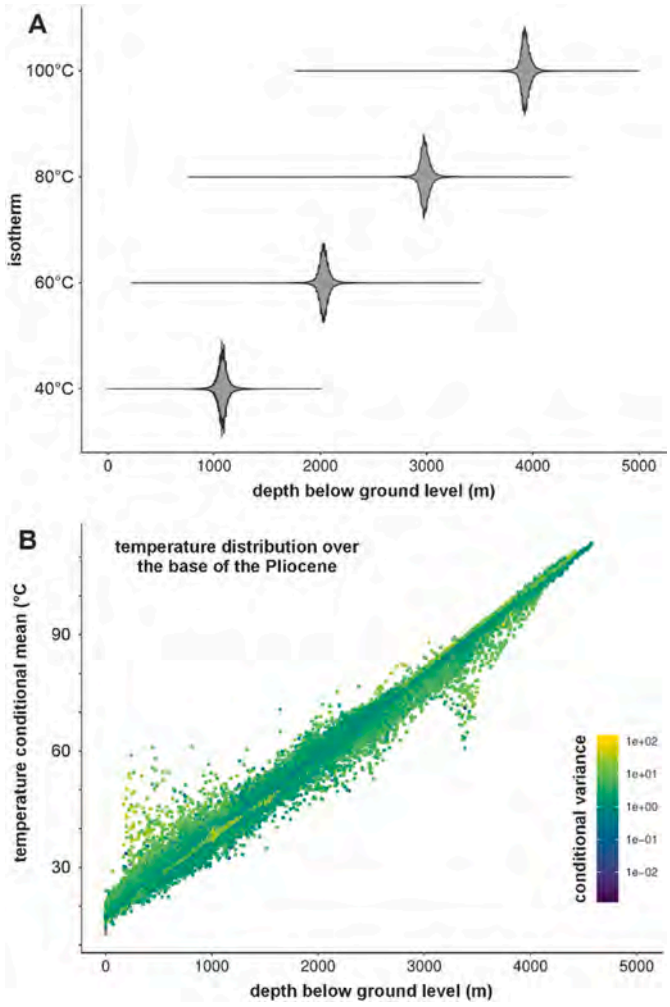

Fig. 8. (A) Violin plots describing the distributions (as kernel density estimation) of depths at which selected isotherms (40, 60, 80 and 100 °C) are encountered in the geocellular grid of expected temperature values. (B) Cross-plot illustrating the relationship between expected temperature values and depth for grid cells that contain the base of the Pliocene; dots are color-coded according to the conditional variance in simulated temperature values.

Caputo, 2021) have suggested that there is evidence for thermal convection within the carbonate units associated with the FA, in the eastern Po Plain. This condition can determine a lower-than-average geothermal gradient in the carbonate units, while simultaneously increasing the geothermal gradient in the units above, mostly in the Oligo-Miocene and Plio-Pleistocene. This inference is supported by geothermal gradient variations found by the wells drilled to the depth of the carbonates in the eastern Po Plain (Fig. 4). This mechanism would explain the highest temperatures found in the FA area, since this is the arc with the largest thrust displacement, as shown in the well Casaglia 1.

Despite the lack of carbonate-cored anticlines at shallow depths in the SA, positive temperature anomalies can be outlined in this area. These anomalies might reflect heat ascent by advection and conduction from hot aquifers hosted in deep carbonate units to the overlying Oligo-Miocene and Plio-Pleistocene terrigenous units, which would be facilitated by fluid migration through faults and fractures, as noted by the anomalies found around the wells Seregna 3 and Villafortuna 1. Notably, the well Seregna 3 shows an increase in geothermal gradient along the section penetrating the carbonate units; instead, the Villafortuna 1 well shows a gradient inversion of smaller magnitude than the one seen in the Casaglia 1 well. This inversion of the gradient could be an indication of convective flow in the aquifer hosted in the carbonates of the Villafortuna structure, in opposition to the proposed mechanism for the rest of the anomalies found in the SA. For both the Villafortuna and the Ferrara structures, the anomalies tend to be localized around the hinge of the anticlines. In some cases, this geometry may reflect a local control by the presence, over certain depths, of fracture corridors aligned along the hinge of the structure, which would facilitate the convection of hot fluids through extensive fracture networks. Fractures play an important geological role in controlling the migration, distribution and accumulation of fluids in hydrothermal systems (Questiaux et al., 2010; Jolie et al., 2021; Fadel et al., 2023). Additionally, the amplitude of thermal anomalies may be partly determined by the dip of faults, with reverse faults being associated with the widest lateral amplitudes of anomalies distributed along anticline hinges (Frottier et al., 2023).

The well Lacchiarella 2, to the west of the EA also displays an increase in the geothermal gradient along its section through the carbonate units, displaying a local thermal anomaly. This could be explained by the inversion structure mentioned above, which displaces the carbonate units bringing their top at depths of ca. 3 km below a very thinned Oligo-Miocene succession, instead of more than ca. 6 km depth top of carbonates as found in the main EA.

To harness the thermal anomaly of the FA, a geothermal plant in Ferrara has been operating since the 1990s, after repurposing the Casaglia 1 well. This borehole was first drilled as an exploratory oil well by Agip (now ENI); even though it was proved dry for hydrocarbons, it led to the discovery of a large geothermal field with water as hot as 100 °C at about 1000 m. Water is extracted at rates varying from 400 m^3/h to 200 m^3/h in winter and summer, respectively. The plant operates as a district-heating system for the municipality of Ferrara and meets all heat demands of the network during the warm season and most of the heat demand for the cold season. The thermal energy supplied to the network from the geothermal plant accounts for 61.6 GWh and the production temperature of 100 °C has remained stable after more than 30 years of exploitation (Manente et al., 2019). This plant is a district-heating geothermal facility for the direct use of a medium-enthalpy geothermal resource. Our model predicts that further exploration of similar geothermal fields could be carried out in the FA using the spatial distribution of the thermal anomaly illustrated in the proposed depth-to-the-isotherm maps, especially in the frontal thrusts where the carbonate units have been displaced at shallow depths.

The exploitation of geothermal resources has proven attractive also outside the FA sector, especially in the SA area. The Rodigo 1 well, near Mantua, is located in one of the areas where the evaluated isotherms tend to be relatively depressed, right in the center of the study area (Fig. 5). This borehole was drilled in the 1970s by Agip (now ENI) for scopes of oil and gas exploration; although it was proven dry, it enabled the discovery of a geothermal reservoir providing water at a rate of 80 m^3/h at 59 °C at a depth below 3000 m. In a joint project involving the University of Milan, Agip (now ENI), and the Mantua district, a plant for using geothermal waters to provide heat for greenhouses and aquacultures was built. The complex has an area of 21,000 m^2 with greenhouses for horticulture and floriculture, drying facilities, and aquaculture tanks, all heated by using the heat of the geothermal reservoir (Facchini et al., 1993). The geothermal complex of Rodigo is another example of the successful use of wells originally drilled for oil and gas and converted to low-enthalpy geothermal wells, producing heat for direct use in agricultural and industrial processes. More recently, several studies have been undertaken (Soldo et al., 2020; Gizzi et al., 2021) to evaluate the conversion of decommissioned oil wells into geothermal wells, specifically in the Villafortuna-Trecate field in the north-western Po-Plain; in particular, it has been proposed that these wells are repurposed for closed-loop circuits for district heating.

Even if drilling deeper than 3000 m might prove uneconomical, as is the case in the main Emilian Arc, the advances in technologies for direct-heat utilization have improved to the point that the minimum production temperature viable for greenhouse heating may be as low as 40 °C (Ultra-Low Temperature District Heating or ULTDH); for district heating

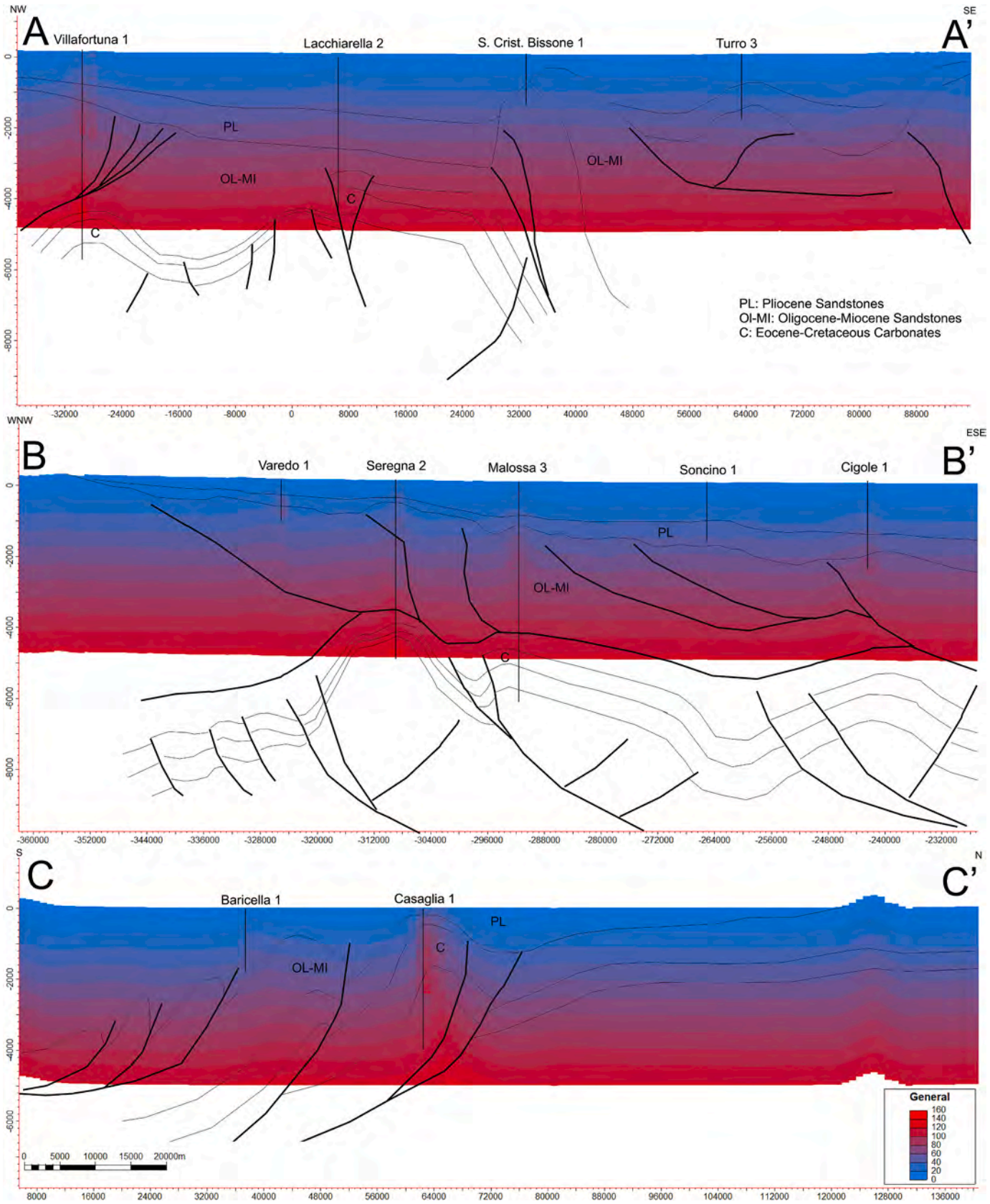

Fig. 9. Cross-sections illustrating relationships between the conditional expectation estimates of the temperature field and surfaces representing both geological structures and stratigraphic boundaries (based on Fantoni and Franciosi, 2010); see Fig. 1 for the location of the sections. Stratigraphic units: PS= Pleistocene units, PL= Pliocene units, O-M= Oligo-Miocene units, C= Carbonate units (Eocene-Cretaceous). Vertical exaggeration ×5.

and cooling, instead, suitable conditions might envisage production temperatures as low as 60 °C (Low-Temperature District Heating or LTDH) with an average surface temperature of 10–15 °C (Limberger et al., 2018; Pomianowski et al., 2020). Large-scale programs of district heating or domestic heating and cooling can also be implemented using ground-source heat pumps at shallower levels with temperatures lower than 40 °C (Mustafa Omer, 2008); this may be particularly applicable to areas like the EA, where important thermal anomalies are not predicted.

6. Conclusions

The Po Plain lies on a complex sedimentary basin placed on the shared foreland of two mountain ranges, the Southern Alps and the Northern Apennines, and characterized by thrusts verging in opposite directions buried by a thick Plio-Pleistocene clastic succession. This configuration has given rise to multiple structural and stratigraphic hydrocarbon traps that have been explored and exploited since the 1940s. However, the maturity of these fields and a policy shift in favor of renewable energy sources have spurred investment in the exploration of geothermal energy. Thanks to decades of oil and gas exploration and production in the area, there exists a vast database of wells with thermal and stratigraphical data. These data, obtained from 743 wells, have been analyzed to produce the first tridimensional geostatistical model of expected temperatures in the Po Plain subsurface at a basin scale. Consideration of the structural and stratigraphic framework allowed us to confirm that certain positive thermal anomalies are associated with structural highs and that the higher temperatures in the Pliocene sedimentary cover tend to occur in the southeastern Po Plain. The structural highs are associated with the SA buried thrusts in the northwest, the reactivated faults of the EA in the mid-west, and the shallow carbonate anticlines of the FA in the southeast. The highest positive thermal anomalies are found at the FA, where the main thrusts have caused the higher displacement of the Mesozoic carbonate units; those units host aquifers subjected to thermal convection, which lowers the geothermal gradient in the carbonates whilst increasing it in the overlying units. Although deeper seated, other thermal anomalies have been found associated with structural highs, which are inferred to be related to hot water migrating from the Mesozoic carbonate aquifers through faults cutting into the Oligo-Miocene and Plio-Pleistocene units.

The evaluation of predicted temperatures at the base of the Pliocene permits to establish that the sedimentary units above the Miocene tend to reach temperatures higher than 80 °C only in the FA area, but also that temperatures just below 60 °C can be found at relatively shallow depths even in the SA area, where several oil wells have been drilled (e.g., Villafortuna-Trecate, Malossa fields). The derived insight can be employed to establish the type of geothermal application (heating and cooling *versus* direct energy production) that may suit a specific sector. The results demonstrate that, at best, the Po Plain exhibits potential for medium- to low-enthalpy geothermal use, mostly for heating purposes, in the units immediately overlying the carbonate units, with the best prospects located along the FA, where exploration efforts should be focused on the structures involving the carbonate units in the core of the anticlines and close to the surface. Notable low-enthalpy resources are expected along the SA buried thrusts, which can be exploited by the conversion of decommissioned oil and gas wells reaching sufficiently high temperatures at economic depths, and which can be exploited for agricultural and district heating purposes. Furthermore, especially in the shallower Plio-Pleistocene sedimentary units of the EA, ground-source heat pumps can be readily deployed for heating and cooling individual buildings, greenhouses, aquaculture activities, or small industries, reducing considerably the need for gas or other non-renewable sources of energy. The outputs of this study can also be employed to guide the exploration of higher-temperature reservoirs at shallow depths, hosted in Oligo-Miocene units. The depth-to-the-isotherm maps carried out in this study at a regional scale can be used as a first-level analysis for further and more detailed local assessment of the positive thermal anomalies. 3D reconstructions of buried geological structures and of the basin architecture can play a pivotal role in the energy transition.

CRediT authorship contribution statement

Daniel Barrera Acosta: Writing – original draft, Methodology, Investigation, Formal analysis, Data curation, Conceptualization. **Giovanni Toscani:** Writing – review & editing, Writing – original draft, Validation, Supervision, Methodology, Conceptualization. **Luca Colombera:** Writing – review & editing, Writing – original draft, Validation, Methodology, Formal analysis, Conceptualization. **Chiara Amadori:** Writing – review & editing, Methodology. **Roberto Fantoni:** Writing – review & editing, Supervision, Conceptualization. **Andrea Di Giulio:** Writing – review & editing, Supervision, Project administration, Conceptualization.

Declaration of competing interest

The authors declare that they have no known competing financial interests or personal relationships that could have appeared to influence the work reported in this paper.

Data availability

Data will be made available on request.

Acknowledgments

This paper is a result of the PON-Ph.D. project of D. Barrera Acosta granted by MUR and the University of Pavia, with support from ENI, towards whom we are grateful. LC, GT and ADG have been supported by a PRIN 2022 PNRR grant (P2022PHWM4), funded by the European Union – Next Generation EU. GT was also supported by a PRIN 2020 grant (2020WA73EM). This research has been supported by the funds of the CARG – Project – Geological Map of Italy 1:50,000" (Foglio 160 Pavia) All the data used for this paper come from public sources (ViDEPI and Geothopica project) and the responsibility for their interpretation rests exclusively with the authors. Seequent is kindly acknowledged for providing the academic licenses of Leapfrog (www.seequent.com); Petroleum Experts (www.petex.com) provided the academic licenses of the Move Suite. Schlumberger (https://www.software.slb.com/products/petrel) provided the academic licenses of Petrel. Two anonymous reviewers are thanked for their constructive comments, which helped us improve the article.

Appendix A. Supplementary data

Supplementary data to this article can be found online at https://doi.org/10.1016/j.marpetgeo.2024.106936.

References

Amadori, C., Garcia-Castellanos, D., Toscani, G., Sternai, P., Fantoni, R., Ghielmi, M., Di Giulio, A., 2018a. Restored topography of the Po Plain-Northern Adriatic region during the Messinian base-level drop—implications for the physiography and compartmentalization of the palaeo-Mediterranean basin. Basin Res. 30 (6), 1247–1263. https://doi.org/10.1111/bre.12302.

Amadori, C., Fantoni, R., Ghielmi, M., Toscani, G., Di Giulio, A., 2018b. 14.C- Po plain-MSC surfaces (2). In: Lofi, J. (Ed.), Seismic Atlas of the Messinian Salinity Crisis markers in the Mediterranean Sea. Volume 2. Mémoires de la Société Géologique de France. Commission for the Geological Map of the World, p. 50. https://doi.org/10.10682/2018MESSINV2. ISBN 9782917310373.

Amadori, C., Toscani, G., Di Giulio, A., Maesano, F.E., D'Ambrogi, C., Ghielmi, M., Fantoni, R., 2019. From cylindrical to non-cylindrical foreland basin: Pliocene–Pleistocene evolution of the Po Plain–Northern Adriatic basin (Italy). Basin Res. 31 (5), 991–1015. https://doi.org/10.1111/bre.12369.

Amadori, C., Ghielmi, M., Mancin, N., Toscani, G., 2020. The evolution of a coastal wedge in response to Plio-Pleistocene climate change: the Northern Adriatic case. Mar. Petrol. Geol. 122 https://doi.org/10.1016/j.marpetgeo.2020.104675.

Amadori, C., Maino, M., Marini, M., Casini, L., Carrapa, B., Jepson, G., Hayes, R.G., Nicola, C., Reguzzi, S., Di Giulio, A., 2023. The role of mantle upwelling on the thermal history of the Tertiary-Piedmont Basin at the Alps-Apennines tectonic boundary. Basin Res. https://doi.org/10.1111/bre.12752.

Bargiacchi, E., Conti, P., Manzella, A., Vaccaro, M., Cerutti, P., Cesari, G., 2021. Thermal Uses of Geothermal Energy, Country Update for Italy.

Bertani, R., Magrini, M., 2000. Enel Geothermal Database. Proceedings World Geothermal Congress, Kvushu-Tohoku, Japan.

Caers, J., 2000. Adding local accuracy to direct sequential simulation 1. Math. Geol. 32 (Issue 7).

Carminati, E., Doglioni, C., 2012. Alps vs. Apennines: the paradigm of a tectonically asymmetric Earth. Earth Sci. Rev. 112 (Issues 1–2), 67–96. https://doi.org/10.1016/j.earscirev.2012.02.004.

Casero, P., 2004. Structural setting of petroleum exploration plays in Italy. Special Volume of the Italian Geological Society for the IGC 32 Florence 189–199.

Casero, P., Rigamonti, A., Iocca, M., 1990. Paleogeographic relationships during Cretaceous between the northern Adriatic area and the eastern southern Alps. Mem. Soc. Geol. It 45, 807–814.

Castellarin, A., 2001. Alps-apennines and Po plain-frontal Apennines relations. Anatomy of an Orogen: the Apennines and Adjacent Mediterranean Basins, pp. 177–196.

Cataldi, R., Mongelli, F., Squarci, P., Taffi, L., Zitot, G., Calore, C., 1995. Geothermal ranking of Italian Territory, 24 (Issue 1).

Cazzini, F., 2018. The history of the upstream oil and gas industry in Italy. Geol. Soc. Spec. Publ. 465 (1), 243–274. https://doi.org/10.1144/SP465.2. Geological Society of London.

Cazzini, F., Dal Zotto, O., Fantoni, R., Ghielmi, M., Ronchi, P., Scotti, P., 2015. Oil and gas in the Adriatic foreland, Italy. J. Petrol. Geol. 38, 255–279.

Dalla Longa, F., Nogueira, L.P., Limberger, J., Wees, J. D. van, van der Zwaan, B., 2020. Scenarios for geothermal energy deployment in Europe. Energy 206. https://doi.org/10.1016/j.energy.2020.118060.

Deming, D., 1994. Estimation of the thermal conductivity anisotropy of rock with application to the determination of terrestrial heat flow. J. Geophys. Res. 99 (B11) https://doi.org/10.1029/94jb02164.

Dercourt, J., Zonenshain, L.P., Ricou, L.E., Kazmin, V.G., Le Pichon, X., Knipper, A.L., Grandjacquet, C., Sbortshikov, I.M., Geyssant, J., Lepvrier, C., Pechersky, D.H., Boulin, J., Sibuet, J.C., Savostin, L.A., Sorokhtin, O., Westphal, M., Bazhenov, M.L., Lauer, J.P., Biju-Duval, B., 1986. Geological evolution of the tethys belt from the Atlantic to the Pamirs since the LIAS. Tectonophysics 123 (1–4), 241–315. https://doi.org/10.1016/0040-1951(86)90199-X.

Di Giulio, A., Mancin, N., Martelli, L., Sani, F., 2013. Foredeep palaeobathymetry and subsidence trends during advancing then retreating subduction: the Northern Apennine case (Oligocene-Miocene, Italy). Basin Res. 25 (3), 260–284. https://doi.org/10.1111/bre.12002.

EGEC, 2021. Geothermal market report key findings. https://www.egec.org/media-publications/egec-geothermal-market-report-2021/.

Facchini, U., Magnoni, S., Sordelli, C., 1993. Rodigo 1, Northern Italy: A Geothermal Complex For Agriculture. Geothermics 22 (2), 135–147.

Fadel, M., Meneses Rioseco, E., Bruna, P.O., Moeck, I., 2023. Pressure transient analysis to investigate a coupled fracture corridor and a fault damage zone causing an early thermal breakthrough in the North Alpine Foreland Basin. Geoenergy Science and Engineering 229.

Fantoni, R., 2017. Mesozoic petroleum system of the Adriatic foreland. Journal of Mediterranean Earth Sciences 9, 151–156.

Fantoni, R., Franciosi, R., 2010. Tectono-sedimentary setting of the Po plain and Adriatic foreland. Rendiconti Lincei 21 (Suppl. 1), 197–209. https://doi.org/10.1007/s12210-010-0102-4.

Fantoni, R., Bersezio, R., Forcella, F., 2004. Alpine structure and deformation chronology at the southern Alps-Po Plain border in Lombardy. Italian Journal of Geosciences 123 (3), 463–476.

Frottier, L., Milesi, G., Roche, V., Duwiquet, H., Taillefer, A., 2023. Heat flow, thermal anomalies, tectonic regimes and high-temperatures geothermal systems in fault zones. Compt. Rendus Geosci. 356 (S2), 1–33.

Ghielmi, M., Minervini, M., Nini, C., Rogledi, S., Rossi, M., Vignolo, A., 2010. Sedimentary and tectonic evolution in the eastern Po-plain and northern Adriatic Sea area from Messinian to middle pleistocene (Italy). Rendiconti Lincei 21 (Suppl. 1), 131–166. https://doi.org/10.1007/s12210-010-0101-5.

Ghielmi, M., Minervini, M., Nini, C., Rogledi, S., Rossi, M., 2013. Late Miocene-Middle Pleistocene sequences in the Po Plain - northern Adriatic Sea (Italy): the stratigraphic record of modification phases affecting a complex foreland basin. Mar. Petrol. Geol. 42, 50–81. https://doi.org/10.1016/j.marpetgeo.2012.11.007.

Gizzi, M., Taddia, G., Lo Russo, S., 2021. Reuse of decommissioned hydrocarbon wells in Italian oilfields by means of a closed-loop geothermal system. Appl. Sci. 11 (5) https://doi.org/10.3390/app11052411.

GSE, 2020. Rapporto Statistico 2020 Energia Da Fonti Rinnovabili in Italia.

ISPRA, 2015. Modello Geologico 3D e Geopotenziali della Pianura Padana Centrale (Progetto GeoMol). In: Rapporti ISPRA, vol. 234. ISSN: 978-88-448-0753-5.

Jolie, E., Scott, S., Faulds, J., Chambefort, I., Axelsson, G., Gutierrez-Negrin, L.C., Rgenspurg, S., Ziegler, M., Ayling, B., Richter, A., Zemedkun, M., 2021. Geological controls on geothermal resources for power generation. Nat. Rev. Earth Environ. 2 (5), 1–16.

Limberger, J., Boxem, T., Pluymaekers, M., Bruhn, D., Manzella, A., Calcagno, P., Beekman, F., Cloetingh, S., van Wees, J.D., 2018. Geothermal energy in deep aquifers: a global assessment of the resource base for direct heat utilization. Renew. Sustain. Energy Rev. 82, 961–975. https://doi.org/10.1016/j.rser.2017.09.084. Elsevier Ltd.

Livani, M., Scrocca, D., Arecco, P., Doglioni, C., 2018. Structural and stratigraphic control on salient and recess development along a thrust belt front: the northern Apennines (Po plain, Italy). J. Geophys. Res. Solid Earth 123 (5), 4360–4387. https://doi.org/10.1002/2017JB015235.

Lund, J.W., Toth, A.N., 2021. Direct utilization of geothermal energy 2020 worldwide review. Geothermics, p. 90. https://doi.org/10.1016/j.geothermics.2020.101915.

Maesano, F.E., D'Ambrogi, C., Burrato, P., Toscani, G., 2015. Slip-rates of blind thrusts in slow deforming areas: examples from the Po Plain (Italy). Tectonophysics 643, 8–25. https://doi.org/10.1016/j.tecto.2014.12.007.

Maesano, F.E., Zuffetti, C., Abbata, A., D'Ambrogi, C., Bersezio, R., 2024. Quaternary slip-rates probabilistic estimation of Northern Apennines thrust front in the Po Plain (Northern Italy) by integrating surface and subsurface data. Tectonophysics 873, 230227. https://doi.org/10.1016/j.tecto.2024.230227.

Mancin, N., Barbieri, C., Di Giulio, A., Fantoni, R., Marchesini, A., Toscani, G., Zanferrari, A., 2016. The Friulian-Venetian basin II: paleogeographic evolution and subsidence analysis from micropaleontological constraints. Italian Journal of Geosciences 135 (3), 460–473. https://doi.org/10.3301/IJG.2015.34.

Manente, G., Lazzaretto, A., Molinari, I., Bronzini, F., 2019. Optimization of the hydraulic performance and integration of a heat storage in the geothermal and waste-to-energy district heating system of Ferrara. J. Clean. Prod. 230, 869–887. https://doi.org/10.1016/j.jclepro.2019.05.146.

Mustafa Omer, A., 2008. Ground-source heat pumps systems and applications. Renew. Sustain. Energy Rev. 12 (2), 344–371. https://doi.org/10.1016/j.rser.2006.10.003.

Muttoni, G., Rogledi, S., 2003. Onset of major pleistocene glaciations in the Alps. Geological Society of America 31, 989–992.

Panara, Y., Maesano, F.E., Amadori, C., Fedorik, J., Toscani, G., Basili, R., 2021. Probabilistic assessment of slip rates and their variability over time of offshore buried thrusts: a case study in the northern Adriatic Sea. Front. Earth Sci. 9 https://doi.org/10.3389/feart.2021.664288.

Pasquale, V., Chiozzi, P., Gola, G., Verdoya, M., 2008. Depth-time correction of petroleum bottom-hole temperatures in the Po Plain, Italy. Geophysics 73 (6). https://doi.org/10.1190/1.2976629.

Pasquale, V., Chiozzi, P., Verdoya, M., 2013. Evidence for thermal convection in the deep carbonate aquifer of the eastern sector of the Po Plain, Italy. Tectonophysics 594, 1–12. https://doi.org/10.1016/j.tecto.2013.03.011.

Pomianowski, M.Z., Johra, H., Marszal-Pomianowska, A., Zhang, C., 2020. Sustainable and energy-efficient domestic hot water systems: a review. In: Renewable and Sustainable Energy Reviews. Elsevier Ltd. https://doi.org/10.1016/j.rser.2020.109900.

Questiaux, J.M., Couples, D., Ruby, N., 2010. Fractured reservoirs with fracture corridors. Geophys. Prospect. 58, 279–295. https://doi.org/10.1111/j.1365-2478.2009.00810.x.

Rapti, D., Caputo, R., 2021. Environmental and energetic implications of the geothermal anomalies in the eastern Po plain. Italian Journal of Engineering Geology and Environment, Special Issue 195–207. https://doi.org/10.4408/IJEGE.2021-01.S-18.

Ravaglia, A., Seno, S., Toscani, G., Fantoni, R., 2006. Mesozoic extension controlling the Southern Alps thrust front geometry under the Po Plain, Italy: insights from sandbox models. J. Struct. Geol. 28 (11), 2084–2096. https://doi.org/10.1016/j.jsg.2006.07.011.

Remy, N., Boucher, A., Wu, J., 2009. Applied Geostatistics with SGeMS: A Users' Guide. Cambridge University Press, pp. 1–98. http://sgems.sourceforge.net/.

Rossi, M., Minervini, M., Ghielmi, M., Rogledi, S., 2015. Messinian and Pliocene erosional surfaces in the Po Plain-Adriatic Basin: insights from allostratigraphy and sequence stratigraphy in assessing play concepts related to accommodation and gateway turnarounds in tectonically active margins. Mar. Petrol. Geol. 66, 192–216. https://doi.org/10.1016/j.marpetgeo.2014.12.012.

Sbrana, A., Marianelli, P., Pasquini, G., Costantini, P., Palmieri, F., Ciani, V., Sbrana, M., 2018. The integration of 3D modeling and simulation to determine the energy potential of low-temperature geothermal systems in the Pisa (Italy) sedimentary plain. Energies 11 (6). https://doi.org/10.3390/en11061591.

Scardia, G., Festa, A., Monegato, G., Pini, R., Rogledi, S., Tremolada, F., Galadini, F., 2015. Evidence for late Alpine tectonics in the Lake Garda area (northern Italy) and seismogenic implications. Bull. Geol. Soc. Am. 127 (1–2), 113–130. https://doi.org/10.1130/B30990.1.

Soldo, E., Alimonti, C., Scrocca, D., 2020. Geothermal repurposing of depleted oil and gas wells in Italy. https://doi.org/10.3390/wef-06907.

Stefani, C., 2002. Variation in terrigenous supplies in the upper Pliocene to recent deposits of the Venice area. Sediment. Geol. 43–55. www.elsevier.com/locate/sedgeo.

Stefani, C., Fellin, M.G., Zattin, M., Zuffa, G.G., Dalmonte, C., Mancin, N., Zanferrari, A., 2007. Provenance and paleogeographic evolution in a multi-source foreland: the Cenozoic Venetian-Friulian Basin (NE Italy). J. Sediment. Res. 77 (11–12), 867–887. https://doi.org/10.2110/jsr.2007.083.

Torri, G., Molinari, F., Martini, A., 2015. Risultati: i geopotenziali dell'area pilota italiana Modello di Temperatura. https://www.isprambiente.gov.it/files/notizie-ispra/notizie-2015/geomol/7_GeoMol_Molinari-Torri.pdf.

Toscani, G., Bonini, L., Ahmad, M.I., Bucci, D. Di, Giulio, A. Di, Seno, S., Galuppo, C., 2014. Opposite verging chains sharing the same foreland: kinematics and interactions through analogue models (Central Po Plain, Italy). Tectonophysics 633 (1), 268–282. https://doi.org/10.1016/j.tecto.2014.07.019.

Toscani, G., Marchesini, A., Barbieri, C., Di Giulio, A., Fantoni, R., Mancin, N., Zanferrari, A., 2016. The Friulian-Venetian basin I: architecture and sediment flux into a shared foreland basin. Italian Journal of Geosciences 135 (3), 444–459. https://doi.org/10.3301/IJG.2015.35.

Tosi, L., Teatini, P., Brancolini, G., Zecchin, M., Carbognin, L., Affatato, A., Baradello, L., 2015. Three-dimensional analysis of the plio-pleistocene seismic sequences in the Venice lagoon (Italy). J. Geol. Soc. 169, 507–510.

Trumpy, E., Manzella, A., 2017. Geothopica and the interactive analysis and visualization of the updated Italian National Geothermal Database. Int. J. Appl. Earth Obs. Geoinf. 54, 28–37. https://doi.org/10.1016/j.jag.2016.09.004.

Turrini, C., Lacombe, O., Roure, F., 2014. Present-day 3D structural model of the Po Valley basin, Northern Italy. Mar. Petrol. Geol. 56, 266–289. https://doi.org/10.1016/j.marpetgeo.2014.02.006.

Turrini, C., Toscani, G., Lacombe, O., Roure, F., 2016. Influence of structural inheritance on foreland-foredeep system evolution: an example from the Po valley region (northern Italy). Mar. Petrol. Geol. 77, 376–398. https://doi.org/10.1016/j.marpetgeo.2016.06.022.

Horner, D.R. (1951) Pressure Build-Up in Wells. Proceedings of the 3rd World Petroleum Congress, 25-43.